International Geology Review, Vol. 46, 2004, p. 575–594.

Discriminant Analysis Applied to Establish Major-Element Field Boundaries for Tectonic Varieties of Basic Rocks

SALIL AGRAWAL,

Department of Geology, University of Rajasthan, Jaipur 302 004, India

MIRNA GUEVARA,[1] AND SURENDRA P. VERMA

Centro de Investigación en Energía, Universidad Nacional Autónoma de México, Priv. Xochicalco S/no., Temixco, Morelos 62580, Mexico

Abstract

The statistical method of linear discriminant analysis has been applied to distinguish Pliocene to Recent basic rocks on the basis of their major-element composition. Studied basic rock suites are from four tectonic settings: island arc, continental rift, ocean island, and mid-ocean ridge. Field boundaries were derived by computing probability functions replacing the past practice of fitting lines by "eye." Highly successful discrimination diagrams have been obtained. A testing set shows that the rate of correct classification ranges from 76% to 96%, and from 80% to 92% when three and four tectonic groups are considered at a time, respectively. The high potential of this approach to identify different tectonic settings for basic rocks is only reduced by the complex tectonic history shown by a few of the compiled samples, by crustal contamination effects in some basic rock samples, and the similarities of mantle sources tapped in different tectonic settings.

Introduction

OF LATE, THE CONCEPT of classifying igneous rocks into distinct tectonic varieties solely based on field occurrence in different tectonic environments has gained wide acceptance amongst geologists (Wilson, 1989). The tectonic setting of an igneous rock is indicated by using suitable prefixes such as continental arc, island arc, continental rift, ocean island, and mid-oceanic ridge for describing basic rocks. Further, based on the *assumption* that physical parameters and chemical environments of magma generation in various tectonic settings are distinct, numerous attempts have been made to identify differences in the chemical composition of the magmas generated in different tectonic environments. Based on major- and trace-element composition of the magmas, several geochemical tectonic discrimination diagrams have been proposed (Pearce and Cann, 1973; Pearce, 1976, 1982; Pearce et al. 1977, 1984; Pearce and Norry, 1979; Wood et al., 1979; Bachelor and Bowden, 1985; Meschede, 1986; Whalen et al., 1987; Maniar and Piccoli, 1989; Sylvester, 1989; Agrawal, 1995; Vasconcelos-F. et al., 1998, 2001; Verma, 2000). That the objective of these diagrams is not to identify new tectonic settings is obvious from the fact that the same class definitions and names are used in prior (field) and posterior (tectonomagmatic-chemical) classifications. These diagrams provide additional variables that extend the prior (field) classification to such igneous rocks that cannot be classified by means of field evidence alone. Examination of the literature for igneous rocks reveals that geochemical discrimination diagrams are routinely applied for paleotectonic reconstructions.

However, several studies (Thompson et al., 1980; Philpotts, 1985; Arculus, 1987; Duncan, 1987; Myers and Breitkopf, 1989; Wang and Glover, 1992) have shown that often these discrimination diagrams are unable to correctly identify the paleotectonic environments. It must be realized here that the success of the discrimination scheme would depend upon the validity of the geological and statistical assumptions inherent in the diagrams. When we plot our samples of igneous rocks in these discrimination diagrams, we automatically enter into the realm of statistics. We *assume* that the assignment rules (i.e., class boundaries) can be extended beyond the dataset on which the diagram was created—i.e., to the entire population of the igneous rocks. Thus, if the geological assumption regarding existence of

[1]Corresponding author; e-mail: mygg@cie.unam.mx

different tectonic settings as discrete spatial entities having distinct physical and chemical parameters of magma generation which form the basis of *prior* (field) and *posterior* (chemical composition) tectonic classifications of igneous rocks is indeed valid, the above-mentioned discrimination diagram limitations can only result from violation of the statistical assumptions. Examples include, first, inadequacy of the dataset used in the creation of the diagram to represent the population, and secondly, the lack of objectiveness in the formulation of the classification rules (Agrawal, 1999). In fact, in all tectonomagmatic and petrologic discrimination diagrams, the linear field boundaries between the groups, instead of some objective method, have been invariably, explicitly or implicitly, drawn by "eye" (e.g., Pearce, 1976, p. 22; Pearce et al., 1984, p. 969; Rickwood, 1989, p. 256).

Using major-element composition of basic rocks from different tectonic settings, viz., island arc (IA), continental rift (CR), oceanic island (OI), and mid-oceanic ridge (MOR), an attempt has been made in this paper to demonstrate that use of sufficiently large sample size and probability-based rules obtained from linear discriminant analysis for defining the field boundaries can result in creation of highly successful discrimination diagrams.

Data Processing

Chemical analyses of basic rocks were collected from the literature (Appendix 1) from around the world corresponding to four tectonic settings, selected on the basis of their occurrence in distinct plate tectonic environments (Fig. 1). We note that continental arc is a missing set that should have been included. This set was initially included, but the results were discouraging because, on the basis of major-element compositions, it is not feasible to discriminate continental arc basalts from island-arc basalts because they are derived from similar sources and by similar processes. The generation of continental-arc and island-arc basic magmas is a very complicated process and only highly differentiated rocks will give contrasting compositions for these two tectonic settings because of the involvement of different types of underlying crust. To solve the problem for basic rocks, trace elements should be incorporated. Our future work on discriminant analysis will involve more elements.

The database contains 249 samples from island arc basic rocks (IAB; named group 1), 234 samples from continental rift basic rocks (CRB; group 2), 252 samples from ocean-island basic rocks (OIB; group 3), and 424 from mid-oceanic ridge basic rocks (MORB; group 4). Major-element analyses of a total of 1159 samples of basic rocks from the above four tectonic groups (Table 1) have been selected to perform the discriminant analysis.

The samples in the database were chosen according to the following criteria: tectonic setting described explicitly and unambiguously by the author(s), $(SiO_2)_{adj}$ content ≤ 52%, and age Pliocene to Recent. All major-element data were included in the database as well as sample name, locality, tectonic setting, and a reference code to identify the bibliographic source (see Table 1 and Appendix 1). All data were processed employing the Middlemost (1989) recommendation for iron-oxidation ratio adjustment using SINCLAS—a program for computing CIPW norm and rock classification according to the IUGS recommendations (Verma et al., 2002). SINCLAS calculates the sum of the major elements (recalculated to an anhydrous 100% adjusted basis) and compares it to the sum of calculated normative minerals, achieving with this an accuracy of no less than 0.002 (%m/m, equivalent to wt% as commonly known to the geological community)—a salient feature that very few existing computer programs are capable of providing (Verma et al., 2003). Because of these novel features, prior to the discriminant analysis we used SINCLAS for computations. We emphasize the importance of using this computer program under the Middlemost option (and not any other method of calculation) for a correct application of the results of our discriminant analysis to "unknown" samples. Otherwise, the user will obtain inconsistent results.

In order to acquire an improved or unbiased estimate of the performance, the assignment rules obtained by discriminant analysis must be tested with data other than those used to derive the assignment rules. For this purpose, we divided the dataset into two parts, viz., the "training set" used for the discriminant analysis to derive the assignment rules, and the "testing set" used to estimate the performance of the assignment rules obtained from the training set.

Thus, in order to create a "testing set," 25 samples were randomly drawn from each group. The remaining (n – 25) samples in each group constituted the training set. The sample size of the training set and testing set of different group is given in Table 2.

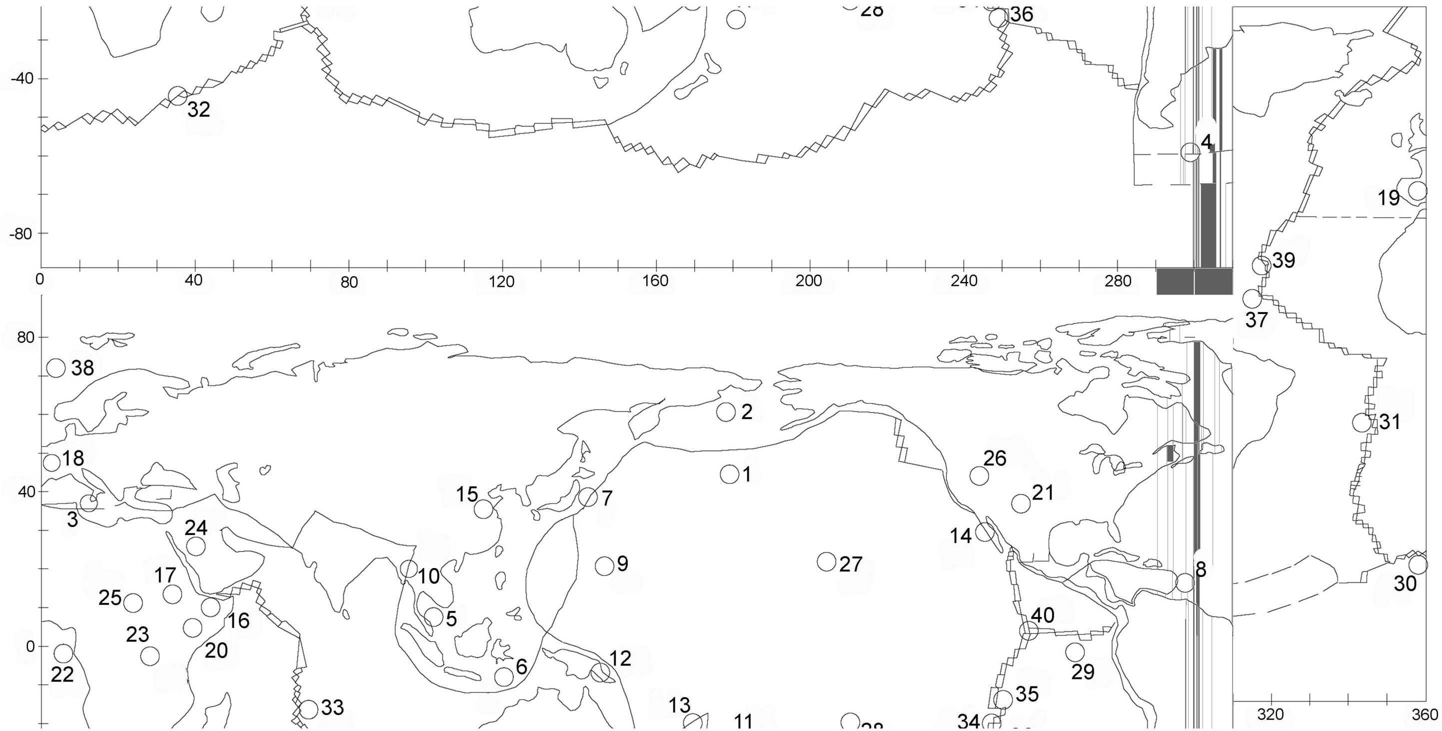

FIG. 1. Location map of the samples included in the database. Details on the sample locations (Loc #) and references are given in Table 1. For the list of literature references for goechemical data from each location see Appendix 1.

TABLE 1. Location, Number of Samples and References for the Samples from Different Tectonic Settings[1]

# Loc.	Location name	Number of samples	Reference
			Island arc[2]
1	Aleutian Islands	36	Brophy, 1986; Kay et al., 1982; Kay and Kay, 1994; Myers et al., 1985, 2002; Nye and Reid, 1986; Romick et al., 1990
2	Alaska	13	Kay and Kay, 1994; Singer et al., 1992a, 1992b
3	Aeolian	11	Francalanci et al., 1993
4	Antarctic	5	Saunders et al., 1980; Smellie, 1983
5	Philippines	27	Bau and Knittel, 1993; Defant et al., 1989; Tatsumi et al., 1992
6	Indonesia, Muriah, Shangihe arc, Sunda arc	52	Edwards et al., 1991; Foden and Varne, 1980; Stolz et al., 1988; Tatsumi et al., 1991; Turner and Foden, 2001; Turner et al., 2003; Wheller et al., 1987; Whitford, 1979
7	Japan, Iwate Volcano, Kuril Arc	25	Kita et al., 2001; Nakada and Karmata, 1991; Nakawa et al., 2002; Sakuyama and Nesbitt, 1986; Tamura, 1994; Togashi et al., 1992
8	Lesser Antilles	18	Arculus, 1976; Brown et al., 1977; Defant et al. 2001; Devine, 1995
9	Mariana Islands	4	Hole et al., 1984; Woodhead, 1988
10	Burma	4	Stephenson and Marshall, 1984
11	New Zealand (Kermadec and Tongan Islands)	25	Bryan et al., 1972; Ewart et al., 1977
12	New Guinea Papua	7	Hegner and Smith, 1992; Woodhead and Johnson, 1993
13	Vanuatu, Australia	22	Barsdell, 1988; Barsdell and Berry, 1990
			Continental rift[3]
14	Baja California	32	Luhr et al., 1995
15	China	26	Chung et al., 1994; Fan and Hooper, 1991; Liu et al., 1992
16	Djibouti	33	Deniel et al., 1994
17	Ethiopia	19	Hart et al., 1989
18	France	12	Chauvel and Jahn, 1984
19	Spain	1	Benito et al., 1999
20	Kenya	28	Class et al., 1994; Le Roex et al., 2001; MacDonald et al., 2001
21	New Mexico	16	Dunker et al., 1991; Johnson and Lipman, 1988; McMillan et al., 2000; Singer and Kudo, 1986
22	Pagalu Island	4	Lee et al., 1994
23	Rwanda, Zaire	32	Aoki et al., 1985; Auchapt et al., 1987; De Mulder et al., 1986
24	Saudi Arabia	13	Camp et al., 1991
25	Sudan	4	Davidson et al., 1989
26	Western U.S.A.	14	Lum et al., 1989

Table continues

TABLE 1. *Continued*

# Loc.	Location name	Number of samples	Reference
		Ocean island[4]	
27	Hawaii	167	Bergmanis et al., 2000; Chen et al., 1990, 1991; Frey et al., 1994; Garcia et al., 1992; Lipman et al., 1990; Maaløe et al., 1992; West et al., 1992
28	French Polynesia	82	Dupuy et al., 1988, 1989; Liotard et al., 1996
29	Galapagos	3	Geist et al., 1986
		Mid-ocean ridge[5]	
30	Antarctica Ridge	10	Le Roex et al., 1981
31	Atlantic Ocean	216	Bryan et al., 1981; Schilling et al., 1983; Le Roex et al., 1987
32	Indian Ridge	26	Dosso et al., 1988; Humler and Whitechurch, 1988; Mahoney et al., 1992
33	Indian Ocean	11	Price et al., 1986
34	Chile Ridge	22	Bach et al., 1996
35	East Pacific Rise	12	Bach et al., 1994
36	Easter microplate, South Pacific	12	Hekinian et al., 1996
37	Mid Atlantic triple junction	9	Bougault et al., 1988
38	Mohns ridge, Norwegian-Greenland sea	8	Haase et al., 1996
39	North Mid-Atlantic Ridge	88	Dosso et al., 1993
40	Triple junction of Pacific-Cocos-EPR	10	Lonsdale et al., 1992

[1]For the complete list of references see Appendix A1.
[2]249 samples: 186 subalkali basalt; 10 picrite; 13 alkali basalt; 15 potassic trachybasalt; 1 tephriphonolite; 1 tephrite, basanite; 12 phonotephrite; 5 tephrite, melanephelinite; 1 basanite, melanephelinite; 3 basaltic trachyandesite, shoshonite; 2 trachybasalt, hawaiite.
[3]234 samples: 64 subalkali basalt; 1 picrite; 85 alkali basalt; 21 potassic trachybasalt; 9 tephrite, basanite; 2 phonotephrite; 3 tephrite, melanephelinite; 7 basanite, melanephelinite; 1 basaltic trachyandesite, shoshonite; 28 trachybasalt, hawaiite; 11 basanite, basanite; 2 basaltic trachyandesite, mugearite.
[4]252 samples: 150 subalkali basalt; 22 picrite; 35 alkali basalt; 4 potassic trachybasalt; 1 tephrite, basanite; 6 basanite, melanephelinite; 10 trachybasalt, hawaiite; 18 basanite, basanite; 2 basaltic trachyandesite, mugearite; 4 meimechite.
[5]424 samples: 412 subalkali basalt; 4 picrobasalt; 7 alkali basalt; 1 trachybasalt, hawaiite.

Comparison of major-element composition of basalt types

Average chemical composition and corresponding standard deviation values of the four tectonic types of basic rocks involved in the present study are presented in Table 3. Study of these data reveals some marked differences in their major-element compositions. The IAB have the highest Al_2O_3, the lowest TiO_2, and relatively low MgO contents. The CRB have low SiO_2 and CaO, and high Fe_2O_3, MnO, Na_2O, K_2O, and P_2O_5. The OIB have the highest TiO_2, FeO, MgO, and the lowest Al_2O_3. The MORB have the highest SiO_2 and CaO and the lowest Na_2O, K_2O, and P_2O_5 amongst the four groups.

An assessment of the within-group and between-group variation in the major-element composition has also been made to evaluate the differences between the group averages given in Table 3. In order to develop a successful discrimination scheme for the four tectonic groups of basic rocks, geochemical variation within the group must be low compared to that between groups.

TABLE 2. Sample Sizes in the Training and Testing sets[1]

Group	Training set	Testing set	Total
IAB (1)	224	25	249
CRB (2)	209	25	234
OIB (3)	227	25	252
MORB (4)	399	25	424
Total	1059	100	1159

[1]IAB = island-arc basic rock; CRB = continental-rift basic rock; OIB = ocean-island basic rock; MORB = mid-ocean ridge basic rock. The numbers in parentheses are group numbers discussed in the text.

TABLE 3. Means and Standard Deviations of Major Elements for Each of the Tectonic Settings[1]

Element	IAB (1) (n = 249)		CRB (2) (n = 234)		OIB (3) (n =252)		MORB (4) (n = 424)	
	mean	s	mean	s	mean	s	mean	s
$(SiO_2)_{adj}$	49.9	1.4	47.6	1.8	48.6	2.5	50.2	0.8
$(TiO_2)_{adj}$	0.91	0.30	2.5	0.7	2.7	0.6	1.42	0.41
$(Al_2O_3)_{adj}$	17.5	2.2	15.0	1.3	13.7	1.8	15.6	1.3
$(Fe_2O_3)_{adj}$	1.69	0.28	2.21	0.41	2.06	0.29	1.69	0.27
$(FeO)_{adj}$	7.8	1.0	9.6	1.3	9.8	1.0	8.4	1.3
$(MnO)_{adj}$	0.180	0.034	0.188	0.026	0.181	0.020	0.175	0.028
$(MgO)_{adj}$	6.8	2.6	7.9	2.2	8.8	3.3	7.9	1.3
$(CaO)_{adj}$	11.2	1.3	9.8	1.4	10.4	1.4	11.7	0.9
$(Na_2O)_{adj}$	2.6	0.7	3.2	0.6	2.6	0.8	2.54	0.41
$(K_2O)_{adj}$	1.2	1.4	1.4	0.9	0.7	0.6	0.23	0.21
$(P_2O_5)_{adj}$	0.25	0.22	0.52	0.22	0.38	0.18	0.16	0.08

[1]Subscript $_{adj}$ refers to the concentrations recalculated to an anhydrous 100% adjusted basis using the computer program SINCLAS employing the Middlemost (1989) recommendation for iron-oxidation ratio adjustment (Verma et al., 2002). Rounding of mean values was done according to the corresponding standard deviation (s) data. Tectonic settings and group numbers are the same as in Table 2. The number of compiled samples (n) is the same as in Table 1 (for rock types, see Table 1).

Table 4 shows Wilk's lambda, sometimes called the U-statistic. When variables are considered individually, the Wilk's lambda is the ratio of the within-group sum of squares to the total sum of squares. A lambda of 1 occurs when all group means are equal. Values close to zero occur when within-group variability is small compared to the total variability. Thus large values of lambda indicate that group means do not appear to be different, whereas small values indicate that group means do appear to be different. The Wilk's lambda values for all major elements except for MgO and MnO are much lower than 1, indicating that group means of these elements are different.

Another statistic given in Table 4 is the significance test for the equality of group means for each major element. For computing the F-ratio statistic, total variation is divided into two components: (a) variation within the group; and (b) variation between the groups. The F values are obtained by dividing the between-group variation by within-group variation. The value of significance given in Table 4 are for "between-group degrees of freedom" df1, which is number of groups minus 1, and "within-group degrees of freedom" df2, which is total number of samples minus number of groups. Because the observed significance level for every major element is less than 0.01 (even <0.0001), the hypothesis that all group means are equal is rejected in each case at the confidence level of 99% (even at the highest confidence level of 99.99%); thus, each element can be considered as a possible candidate for predictor variable in the discriminant analysis.

TABLE 4. Test for Equality of Group Means[1]

Variable	Wilks' Lambda	F-ratio	Significance
$(SiO_2)_{adj}$	0.718	121.1	0.0000
$(TiO_2)_{adj}$	0.310	684.8	0.0000
$(Al_2O_3)_{adj}$	0.579	223.6	0.0000
$(Fe_2O_3)_{adj}$	0.644	170.4	0.0000
$(FeO)_{adj}$	0.685	141.5	0.0000
$(MnO)_{adj}$	0.976	7.6	0.0000
$(MgO)_{adj}$	0.907	31.7	0.0000
$(CaO)_{adj}$	0.752	101.5	0.0000
$(Na_2O)_{adj}$	0.863	48.8	0.0000
$(K_2O)_{adj}$	0.743	106.5	0.0000
$(P_2O_5)_{adj}$	0.602	203.7	0.0000

[1]Wilks' Lambda (U-statistic) and univariate F-ratio with degrees of freedom, df1 = 3 and df2 = 1155.

Discriminant Analysis

In tectonic (field) classifications of igneous rocks, various tectonic varieties, named after different tectonic settings, are distinguished *a priori*. These classes are defined by qualitative field variables, which in turn permit tectonic classification of igneous rocks within the scheme. In geochemical tectonic discrimination schemes, class definitions and names used in the *a priori* (field) classification are retained, and an attempt is made to identify new quantitative, chemical variables that can surrogate for the field variables. The chemical variables make it possible to extend the prior classification to such rocks that cannot be classified due to inconclusive field evidences. Obviously, both the prior (field) and posterior (geochemical) classifications of igneous rocks into tectonic classes, in mathematical terms, are discriminant analyses. Therefore, the statistical technique of linear discriminant analysis has been selected to distinguish the tectonic varieties of basic rocks on the basis of their major-element compositions.

The discriminant analysis is a statistical technique most commonly used to examine how far it is possible to distinguish between members of different, pre-defined, groups, on the basis of observations made upon them. The aim in mathematical terms is to summarize p-dimensional observations from the classes on a one-dimensional linear function or index that discriminates between the classes by some measure of maximum separation, and serves as a basis for classifying samples of unknown classes. Although the concept of discriminant analysis is fairly simple, actual mechanics of computing the same is somewhat involved (see Kendall et al., 1983; Morrison, 1990). Discriminant analysis, however, can be easily performed with standard statistical software. In this work we used the SPSS/PC+ Advanced Statistics Version 4.0 statistical package. A detailed account of the mathematical procedure involved in discriminant analysis is given in Kendall et al. (1983) and Morrison (1990).

As mentioned earlier, in all tectonic discrimination diagrams that are in vogue, group boundaries have been almost invariably drawn by fitting lines by "eye." These purely subjective field boundaries are then used for determining tectonic settings of "unknown" samples. In contrast to this, the use of the linear discriminant analysis provides formal (mathematical) methods of classification having several advantages. For example, the classification rules are objective, the results can be reproduced, the performance of the assignment rules can be subjected to rigorous assessment, and by selecting only those variables that contribute to the power of the discriminant function, the dimensionality of the problem can be reduced. Discriminant analysis provides functions from which discriminant scores for the samples can be computed. When two or more functions are obtained, they can be used to create binary tectonic discrimination diagrams. We note here that the number of discriminant functions when there are g groups and p independent variables (one minus the actual number of data variables in case of closed data) will be either g-1 or p, whichever is smaller.

The major-element analyses in the dataset used in this paper all sum to 100. Aitchinson (1986, 1989), in his pioneering work on the statistical analysis of unit-sum constrained data, has suggested that in case of closed number data, log-ratio transformation should be performed. Rock (1989), on the other hand, has discussed the practical difficulties associated with log-ratio transformation, for example, the extreme difficulty to grasp nature of the concepts, the unavailability of executable algorithms of estimation of log-ratio vectors, and the inapplicability of log-ratio transformation in cases where a variable had zero or a missing value. Further, it must be realized here that log transformation has the effect of assigning less weight to the larger values and more weight to the smaller values in the original data points. Although it may be helpful in constraining values that have extremely dissimilar magnitudes, according to Whitten et al. (1987a), assigning dissimilar (or for that matter equal) weights to various variables can be considered as "subjective," and different geologists might suggest a multitude of different weights for each variable based on their personal geological experiences and biases. In view of the above, in the present analysis no transformation has been applied to the data except for the method of adjustment described above under the heading Data Processing.

Selection of predictor variables

The success of discriminant analysis depends on selection of appropriate predictor variables. Whitten et al. (1987b) have argued that each and every measured variable must be included in the discriminant analysis to make it petrogenetically meaningful. On the other hand, Chayes (1987) warned that including variables that do not contribute to the power of the discriminant function could result in so much "noise" that a petrogenetically meaningful interpretation of the discriminant functions may not be possible. Often, predictor variables are selected on the basis of a significance test (univariate F-ratio) for the null hypothesis that all group means are equal. In fact, Pearce (1976) adopted this approach in creating his discriminant diagrams for tectonic varieties of basalts.

As compared to the above method of selection of predictor variables on the basis of univariate analysis of variance, statistical procedures such as linear discriminant analysis, with emphasis on analyzing all variables together, permit incorporation of important information about the mutual relationships between the variables. In linear discriminant analysis, each raw variable is projected in the form of discriminant functions, and thus, the selection of predictor variables can be based on the test of Wilk's lambda, that in the population means of the *discriminant function* in all the groups are equal. In the present analysis, predictor variables were selected by a stepwise method, with minimization of the Wilk's lambda as the criterion for variable selection. At each step the variable that resulted in the smallest lambda for the discriminant function was selected.

Number of groups considered simultaneously

In tectonic discrimination diagrams often an attempt is made to simultaneously distinguish as many as five groups in the narrow space of two (bivariate diagrams) or three (ternary diagrams) compositional variables. Use of discriminant functions instead of raw variables is advantageous in the sense that each discriminant function can represent several of the compositional variables. However, it must be realized here that even when using bivariate plots of discriminant functions, simultaneous consideration of five or more groups would be an ill-posed problem in view of the difficulties in generalizing the classification rules in mathematical terms, particularly where the groups show overlapping. Thus, the efficiency of the classification rule would increase if two or three groups only were considered at a time. In view of this, although initially all four groups were considered simultaneously, in order to reduce the number of groups taken at a time, discriminant analysis was performed for all combinations of the four groups by taking only four and three groups at a time.

Discriminant score and classification rule

The analysis provided unstandardized linear discriminant function coefficients. Based on the coefficients, the discriminant score of the individual case in each group can be obtained as:

$$D = B_1X_1 + B_2X_2 + \ldots.. + BpXp + B_0, \qquad (1)$$

where X is the major-element value, B is the discriminant function coefficient, and B_0 is a constant. If *g* groups are involved in discriminant analysis, *g* – 1 discriminant functions are obtained; hence the

TABLE 5. Assessment of Correct Classification (%) between the IAB (1), CRB (2), OIB (3), and MORB (4) Groups

Group	Set	*n*	IAB (1)	CRB (2)	OIB (3)	MORB (4)	Overall
1-2-3-4	Training	1059	80.8	70.3	80.6	93.0	83.3
1-2-3-4	Testing	100	84.0	80.0	88.0	92.0	86.0
1-2-3	Training	660	84.0	79.4	79.7		85.0
1-2-3	Testing	75	92.0	88.0	84.0		85.0
1-2-4	Training	832	80.8	84.7		93.5	87.9
1-2-4	Testing	75	88.0	96.0		92.0	92.0
1-3-4	Training	850	84.8		95.6	94.5	92.2
1-3-4	Testing	75	92.0		96.0	92.0	93.3
2-3-4	Training	835		71.8	82.4	97.5	86.9
2-3-4	Testing	75		76.0	88.0	96.0	86.7

number of discriminant functions in three- and four-group discriminant analyses are 2 and 3, respectively. The discriminant scores D1, D2, and D3 were calculated using the above equation. Further, from the discriminant scores, the mean discriminant scores for the groups, known as group centroids, can be calculated.

The rule for classifying a given basic rock sample into one of the tectonic groups can be obtained from its discriminant score *D*. The probability that a basic rock with a discriminant score *D* belongs to group *i* is estimated by:

$$P(Gi/D) = P(D/Gi)\, P(Gi), \tag{2}$$

where P(G*i*/D) is the posterior probability, P(D/G*i*) is the conditional probability, and P(G*i*) is the prior probability.

The prior probability, which is an estimate of the likelihood that a case belongs to a particular group when no information about it is available, has been assumed to be equal for all groups in the present analysis. Furthermore, if the discriminant scores (of the cases used for the analysis) are normally distributed, and the parameters of distribution can be estimated using the mean discriminant scores, it is possible to calculate the probability of obtaining a particular discriminant score value *D* if the case is a member of Group 1 or Group 2, and so on. This probability is called conditional probability P(D/G*i*) of *D* given the group. The case is assumed to belong to a particular group and the probability of the observed score given membership in the group is estimated. From the prior and conditional probabilities, the posterior probability P(G*i*/D) can be estimated using Bayes' rule. A case is classified, based on its discriminant score *D*, in the group for which the posterior probability is largest (see Morrison, 1990, for further information).

Result of the Discriminant Analysis

Table 5 displays the result of the discriminant analysis using the training set of the IAB, CRB, OIB, and MORB groups. The discriminant analysis was performed five times to consider the four tectonic groups of basic rocks and all possible combinations of three groups taken at a time. In each analysis, the predictor variables were selected by the criterion of reduction of Wilk's lambda for the discriminant function. Further, considering the testing set as "unknown" cases, the assignment rules obtained from the discriminant analysis of the training set were used to classify samples comprising the testing set. The rates of correct classification obtained for the testing set are also given in Table 5. The first column of the table indicates which groups were involved in the analysis, and the third column gives

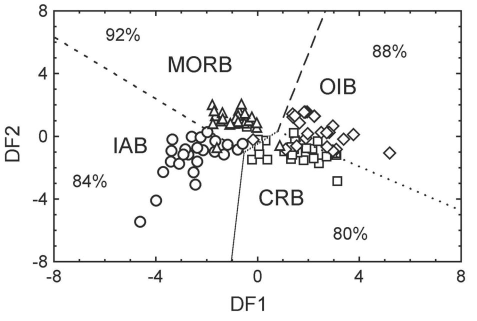

FIG. 2. Diagram IAB-CRB-OIB-MORB displaying samples of the testing set. The symbols used for plotting the testing set samples are: open circles = IAB; open squares = CRB; open rhombus = OIB, open triangle = MORB. The coordinates (DF1, DF2) of the field boundaries between different tectonic settings are as follows: (–1.03, –8.00) and (–0.52, –0.99) for the boundary IAB-CRB; (0.80, 0.32) and (8.00, –4.75) for CRB-OIB; (0.80, 0.32) and (2.67, 8.00) for OIB-MORB; (–0.52, –1.03) and (–8.00, 6.33) for IAB-MORB; and (–0.52, –1.03) and (0.80, 0.32) for CRB-MORB. The percentages shown in this figure refer to the percentage of the correct classification for samples of the testing set (see Table 5). Discriminant function coefficients are displayed in Table 6; i.e., for computing the discriminant functions DF1 and DF2 for "unknown" samples use equations (3) and (4) in the text (note the discriminant function coefficients, i.e., the multiplication factors for major elements are listed in Table 6).

the total number of samples. In the fourth to seventh columns the success rate of the discriminant analysis is given in terms of percentage of correct classification of the cases in each tectonic group. The last column gives overall rate of correct classification achieved in discriminant analysis for that particular combination of groups.

Perusal of Table 5 for the training set reveals that: (1) the rate of correct classification for the samples in the IAB group shows the highest value (84.8%) when IAB, OIB, and MORB groups are considered simultaneously; (2) the CRB group yields the highest rate (84.7%) of correct classification in the discriminant analysis involving IAB-CRB-MORB groups, which is significantly higher than the 70.3% rate of correct classification obtained in the four-group discriminant analysis of IAB-CRB-OIB-MORB groups; (3) the samples of the OIB group show the highest rate (95.6%) of correct classification when the groups IAB-OIB-MORB are analyzed together and the lowest rate (79.7%) for the set IAB-CRB-OIB; (4) the MORB samples show consistently high rates of correct classification (>90%) in all combinations of the groups. The highest rate of correct classification for the MORB group is 97.5%, achieved in the discriminant analysis involving CRB-OIB-MORB groups.

It is also obvious from Table 5 that the overall rate of correct classification increases when the number of groups taken for discrimination is reduced from four to three. The high rates of correct classification obtained for individual groups clearly demonstrate the potential of discriminant analysis to identify basic rocks belonging to different tectonic settings on the basis of major-element compositions.

It must be realized here that the assignment rules obtained in the discriminant analysis are based on the characteristics exhibited by the samples (training set) used in the analysis, and designed to minimize mis-classification in the training set. Therefore, it is generally expected that unless the data used in discriminant analysis (i.e., in the training set) are perfectly representative of the population, the resulting classifier may perform poorly with respect to the population as a whole. In view of this, the classification results of the testing set are most interesting. It may be recalled here that cases in the testing set were not included in the dataset used for obtaining the classification rules (training set), and thus the rates of correct classification obtained on the testing set provide a realistic estimate of the performance of the classification rules for the entire population of basic rocks, i.e., for future applications to "unknown" samples. Perusal of Table 5 reveals that for the tectonic groups IAB, CRB, and OIB, the rates of correct classification obtained in the testing set are higher than the corresponding training set. In the case of the MORB group, although the testing set gives marginally lower rates of correct classification, very high rates of correct classification (92% or more) have been consistently obtained. Most promising are discriminant analyses where only three groups are considered at a time, because high overall rates of 85.0% to 93.3% correct classification have been obtained for both the training and testing sets.

Discrimination between IAB-CRB-OIB-MORB groups

Based on the above results, an attempt has been made to develop a discrimination scheme for the four tectonic types of basic rocks, namely, IAB, CRB, OIB, and MORB. The scheme consists of five diagrams (Figs. 2 and 3A–3D). Figure 2 includes all the four tectonic types of basic rocks, whereas discrimination between three groups has been integrated in Figures 3A–3D. Thus, each tectonic group appears in four of these diagrams, which are plots of the two discriminant functions, DF1 and DF2, respectively. Use of the discriminant function for displaying the variations between the groups is advantageous because the discriminant functions maximize the between-group variations of the raw variables, and hence reduce the dimensionality of the problem (for example, the 11 major oxide compositional variables are now represented by two discriminant functions). In the four-group discriminant analysis, which resulted in Figure 2, three discriminant functions (g –1; g = 4) were obtained. Amongst these three functions, the first two functions accounted for 97.16% of between-group variability. In view of the insignificance of the third function in terms of between-group variability, the classification rules in Figure 2 are based on the two discriminant functions, DF1 and DF2 only. The form of these functions is:

$$DF1 = 0.258 \cdot (SiO_2)_{adj} + 2.395 \cdot (TiO_2)_{adj} + 0.106 \cdot (Al_2O_3)_{adj} + 1.019 \cdot (Fe_2O_3)_{adj} - 6.778 \cdot (MnO)_{adj} + 0.405 \cdot (MgO)_{adj} + 0.119 \cdot (CaO)_{adj} + 0.071 \cdot (Na_2O)_{adj} - 0.198 \cdot (K_2O)_{adj} + 0.613 \cdot (P_2O_5)_{adj} - 24.065 \quad (3)$$

$$DF2 = 0.730 \cdot (SiO_2)_{adj} + 1.119 \cdot (TiO_2)_{adj} + 0.156 \cdot (Al_2O_3)_{adj} + 1.332 \cdot (Fe_2O_3)_{adj} + 4.376 \cdot (MnO)_{adj} + 0.493 \cdot (MgO)_{adj} + 0.936 \cdot (CaO)_{adj} + 0.882 \cdot (Na_2O)_{adj} - 0.291 \cdot (K_2O)_{adj} - 1.572 \cdot (P_2O_5)_{adj} - 59.472 \quad (4)$$

The discriminant function coefficients for each major element (i.e., the corresponding multiplication factors) are also listed in Table 6.

Similarly, the discriminant function coefficients for the three-group analyses (Fig. 3A–D) are reported in Table 7. It should be noted here that major elements selected in the discriminant functions are not identical in all the diagrams. This is because only those major elements which resulted in minimization of the Wilk's lambda for the discriminant function were selected.

In a significant departure from the past practice of defining the field boundaries between the groups by fitting lines by "eye," the field boundaries in Figures 2 and 3A–3D were derived by computing the posterior probability from discriminant scores D1 and D2. Thus, in Figures 2 and 3A–D, the line separating any two groups represents values of scores D1 and D2 that would yield equal (i.e., 50 percent) posterior probabilities for the two groups, and posterior probability belonging to the other group(s) would be zero. The triple junction of the two group field boundaries in Figures 2 and 3A–3D represents the values of D1 and D2 for which the posterior probability belonging to the three groups is equal, i.e., 33.33%. As we move away from the field boundary, i.e., into the field of a group, the posterior probability becomes highest for that group. The field boundaries in Figures 2 and 3A–3D obviously are projections of the Bayes rule of classification described earlier. Thus, the classification of a case obtained by calculation of posterior probability and by plotting the case in the figures always will be identical. The use of the diagram, however, is advantageous because it eliminates the need for computation of posterior probabilities for unknown cases.

It is interesting to note that the MORB samples form a tight cluster in all the diagrams, whereas IAB, CRB, and OIB samples show wide variations in the discriminant scores, suggesting that crustal processes (such as differentiation or magma contamination) and/or mantle processes (such as chemical

TABLE 6. Discriminant Function Coefficients for the Four Groups IAB-CRB-OIB-MORB[1]

	DF1	DF2
$(SiO_2)_{adj}$	0.258	0.730
$(TiO_2)_{adj}$	2.395	1.119
$(Al_2O_3)_{adj}$	0.106	0.156
$(Fe_2O_3)_{adj}$	1.019	1.332
$(MnO)_{adj}$	–6.778	4.376
$(MgO)_{adj}$	0.405	0.493
$(CaO)_{adj}$	0.119	0.936
$(Na_2O)_{adj}$	0.071	0.882
$(K_2O)_{adj}$	–0.198	–0.291
$(P_2O_5)_{adj}$	0.613	–1.572
Constant	–24.065	–59.472
% of variance	77.83	19.33

[1]The third function obtained in this analysis accounted for the remaining 2.84% of between-groups variance.

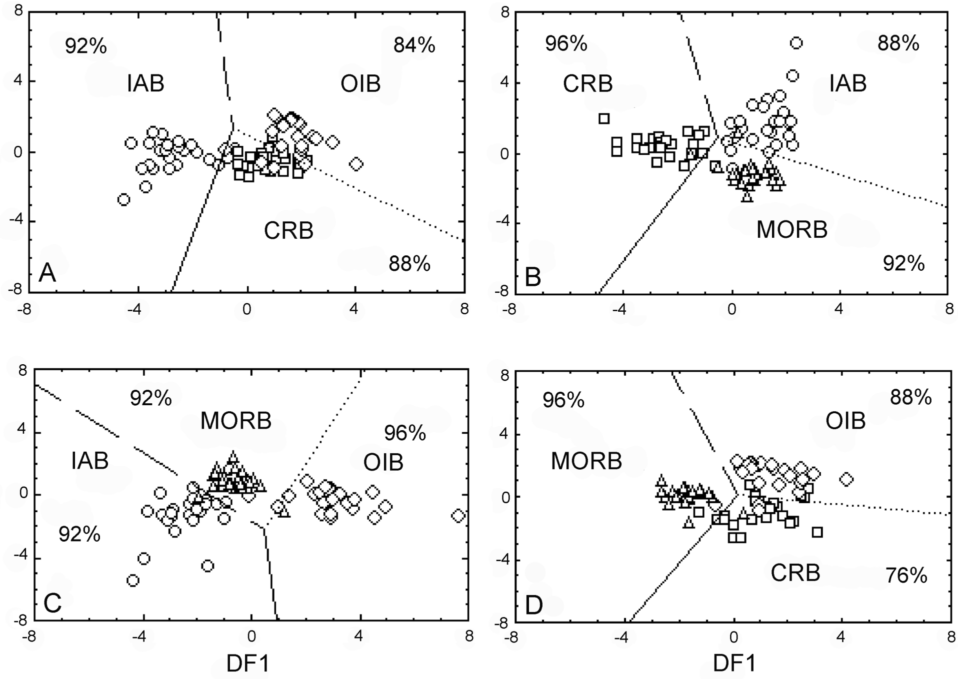

FIG. 3. Diagrams considering three groups at the time (symbols as in Fig. 2) for samples of the testing set. The symbols used for plotting the testing set samples are the same as in Figure 2. The percentages shown refer to the percentage of the correct classification for samples of the testing set (see Table 5). Discriminant function coefficients are shown in Table 7. For computing the functions DF1 and DF2 for "unknown" samples, use the discriminant function coefficients listed in Table 7 for each group of three tectonic settings and construct new equations similar to equations (3) and (4) in the text. As an example, the new equations for the group IAB-CRB-OIB *(1-2-3)* (Fig. 3A) are as follows: [DF1 = 0.251 · $(SiO_2)_{adj}$ + 2.034 · $(TiO_2)_{adj}$ – 0.100 · $(Al_2O_3)_{adj}$ + 0.573 · $(Fe_2O_3)_{adj}$ + 0.032 · $(FeO)_{adj}$ – 2.877 · $(MnO)_{adj}$ + 0.260 · $(MgO)_{adj}$ + 0.052 · $(CaO)_{adj}$ + 0.322 · $(Na_2O)_{adj}$ – 0.229 · $(K_2O)_{adj}$ – 18.974] and [DF2 = 2.150 · $(SiO_2)_{adj}$ + 2.711 · $(TiO_2)_{adj}$ + 1.792 · $(Al_2O_3)_{adj}$ + 2.295 · $(Fe_2O_3)_{adj}$ + 1.484 · $(FeO)_{adj}$ + 8.594 · $(MnO)_{adj}$ + 1.896 · $(MgO)_{adj}$ + 2.158 · $(CaO)_{adj}$ + 1.201 · $(Na_2O)_{adj}$ + 1.763 · $(K_2O)_{adj}$ – 200.276]. Similar equations can be constructed for using the other three diagrams. The corresponding coordinates (DF1, DF2) for plotting field boundaries between different tectonic settings are as follows: A. Group IAB-CRB-OIB *(1-2-3)*: (–0.52, 1.34) and (–2.76, –8.00) for the boundary IAB-CRB; (–0.52, 1.34) and (8.00, –5.11) for CRB-OIB; and (–0.52, 1.34) and (–1.09, 8.00) for IAB-OIB. B. Group IAB-CRB-MORB *(1-2-4)*: (–0.49, 0.84) and (–4.97, –8.00) for the boundary CRB-MORB; (–0.49, 0.84) and (8.00, –3.04) for IAB-MORB; and (–0.49, 0.84) and (–1.93, 8.00) for IAB-CRB. C. Group IAB-OIB-MORB *(1-3-4)*: (0.50, –2.17) and (0.97, –8.00) for the boundary IAB-OIB; (0.50, –2.17) and (4.27, 8.00) for OIB-MORB; and (0.50, –2.17) and (–8.00, 7.10) for IAB-MORB. D. Group CRB-OIB-MORB *(2-3-4)*: (0.17, 0.07) and (–3.83, –8.00) for the boundary CRB-MORB; (0.17, 0.07) and (8.00, –1.17) for CRB-OIB; and (0.17, 0.07) and (–2.28, 8.00) for OIB-MORB.

nature of magma sources, melting regime, etc.), may have an effect on the composition of the basic rocks of these tectonic settings.

Further considerations on mis-classified samples

Advances in analytical techniques imply an improvement in accuracy and precision of quantitative analysis. Unfortunately, still there is no rule that chemical analyses should be reported including *individual* uncertainties. This information would help to discard or retain data according to their quality. Considering that major-element analyses included in the database were made during the past three decades, the uncertainty of analytical data may affect the result of discrimination for those samples that plot near the field boundaries in Figures 2 and 3.

Table 8 presents a summary of the mis-classified samples from the training set as well as the testing set. In Figure 2 (note only samples from the testing

TABLE 7. Discriminant Function Coefficients for the Three Group Discriminant Analyses[1]

	IAB-CRB-OIB (1-2-3)			IAB-CRB-MORB (1-2-4)	
	DF1	DF2		DF1	DF2
$(SiO_2)_{adj}$	0.251	2.150	$(SiO_2)_{adj}$	0.435	0.601
$(TiO_2)_{adj}$	2.034	2.711	$(TiO_2)_{adj}$	–1.392	–0.335
$(Al_2O_3)_{adj}$	–0.100	1.792	$(Al_2O_3)_{adj}$	0.183	1.332
$(Fe_2O_3)_{adj}$	0.573	2.295	$(FeO)_{adj}$	0.148	1.449
$(FeO)_{adj}$	0.032	1.484	$(MnO)_{adj}$	7.690	0.756
$(MnO)_{adj}$	–2.877	8.594	$(MgO)_{adj}$	0.021	0.893
$(MgO)_{adj}$	0.260	1.896	$(CaO)_{adj}$	0.380	0.448
$(CaO)_{adj}$	0.052	2.158	$(Na_2O)_{adj}$	0.036	0.525
$(Na_2O)_{adj}$	0.322	1.201	$(K_2O)_{adj}$	0.462	1.734
$(K_2O)_{adj}$	–0.229	1.763	$(P_2O_5)_{adj}$	–1.192	2.494
Constant	–18.974	–200.276	Constant	–29.435	–78.236
	IAB-OIB-MORB (1-3-4)			CRB-OIB-MORB (2-3-4)	
	DF1	DF2		DF1	DF2
$(SiO_2)_{adj}$	1.232	1.384	$(SiO_2)_{adj}$	0.310	0.703
$(TiO_2)_{adj}$	4.166	1.091	$(TiO_2)_{adj}$	1.936	2.454
$(Al_2O_3)_{adj}$	1.085	0.908	$(Al_2O_3)_{adj}$	0.341	0.233
$(Fe_2O_3)_{adj}$	3.522	2.419	$(Fe_2O_3)_{adj}$	0.760	1.943
$(FeO)_{adj}$	0.500	0.886	$(FeO)_{adj}$	0.351	–0.182
$(MnO)_{adj}$	–3.930	5.281	$(MnO)_{adj}$	–11.315	–2.421
$(MgO)_{adj}$	1.334	1.269	$(MgO)_{adj}$	0.526	0.618
$(CaO)_{adj}$	1.085	1.790	$(CaO)_{adj}$	0.084	0.712
$(Na_2O)_{adj}$	0.416	2.572	$(K_2O)_{adj}$	0.312	–0.866
$(K_2O)_{adj}$	0.827	0.138	$(P_2O_5)_{adj}$	1.892	–1.180
Constant	–119.050	–134.295	Constant	–32.909	–56.455

[1]The two functions (DF1 and DF2) together account for 100% of between-group variance in all the above three-group analyses.

set are plotted in this diagram, and not those from the training set; therefore, refer to Table 8 for details) most mis-classified IAB samples are classified as MORB (39 out of 47 mis-classified samples). This may be due to the possibility that such IAB samples might have originated in a MORB-type mantle with a very small contribution from the subducting slab (fluids/melts), thus rendering their chemistry very similar to MORB chemistry. Similarly, a few mis-classified IAB samples as CRB in Figure 2 (7 out of 47 mis-classified samples; Table 8) may be due to their origin in a relatively enriched mantle that is less depleted than a MORB mantle and an insignificant involvement of fluids or melts from the subducting slab.

Samples from both CRB and OIB tectonic settings may have similar sources with lithospheric and asthenospheric contributions. This is the main

TABLE 8. Synthesis of Number of Mis-classified Samples from Training Set[1] and Testing Set[2]

Using:		Training set					Testing set				
Figure #	Group	IAB	CRB	OIB	MORB	Total	IAB	CRB	OIB	MORB	Total
2	IAB	–	7	1	35	43	–	0	0	4	4
	CRB	4	–	36	22	62	0	–	3	2	5
	OIB	0	42	–	2	44	0	1	–	2	3
	MORB	15	6	7	–	28	1	1	0	–	2
3A	IAB	–	36	0	n.a.	36	–	2	0	n.a.	2
	CRB	5	–	38	n.a.	43	0	–	3	n.a.	3
	OIB	1	45	–	n.a.	46	0	4	–	n.a.	4
3B	IAB	–	8	n.a.	35	43	–	0	n.a.	3	3
	CRB	4	–	n.a.	28	32	0	–	n.a.	1	1
	MORB	13	19	n.a.	–	22	1	1	n.a.	0	2
3C	IAB	–	n.a.	2	32	34	–	n.a.	0	2	2
	OIB	0	n.a.	–	10	10	0	n.a.	–	1	1
	MORB	13	n.a.	9	–	22	1	n.a.	1	–	2
3D	CRB	n.a.	–	33	26	59	n.a.	–	5	1	6
	OIB	n.a.	38	–	2	40	n.a.	2	–	1	3
	MORB	n.a.	4	6	–	10	n.a.	1	0	–	1

[1]IAB (224 samples), CRB (209 samples), OIB (227 samples), and MORB (399 samples).
[2]IAB (25 samples), CRB (25 samples), OIB (25 samples), and MORB (25 samples).
[3]n.a. = not applicable for this diagram.

reason why in Figure 2 most mis-classified CRB samples are classified as OIB (39 out of 67 mis-classified samples; Table 8) and vice versa (43 out of 47 mis-classified samples; Table 8). Similarly, in Figure 2 some CRB mis-classified as MORB (24 out of 67 mis-classified samples; Table 8) may have originated in a depleted mantle similar to a MORB mantle with only a little additional metasomatism in their source region. A still lesser number of CRB and OIB samples that fall in the arc setting (IAB) in Figure 2 (4 out of 114 mis-classified samples; Table 8) might have been contaminated by the crust. A few mis-classified MORB samples in Figure 2 (30 mis-classified samples; Table 8) owe their origin to the similar mechanisms as those put forth above for the mis-classification of other tectonic types. Similar reasoning is valid for the mis-classifications observed in Figures 3A–3D (Table 8).

Thus, the high potential of the discriminant analysis approach to identify different tectonic settings for basic rocks is only reduced by the complex tectonic history shown by a few of the mis-classified samples. Another reason is that some basic rocks have characteristics that suggest involvement of crustal contamination. Finally, the mantle sources for some samples from different tectonic settings in some cases are similar. The knowledge of major- and trace-element chemistry, field observation, petrography, and tectonic history can help to explain the mis-classified cases.

Using the discrimination diagrams for classifying "unknown" samples

In order to use the diagrams (Figs. 2 and 3A–3D), the major-element composition of the basic rocks *must* first be adjusted by the same method applied to the data bank used in this analysis. Thereafter, using the adjusted major-element analyses (i.e., those obtained from the computer program SINCLAS; Verma et al., 2002), the values of discriminant scores D1 and D2 for each sample can be computed from the discriminant functions DF1 and DF2 given in Tables 6 and 7 and plotted in Figures 2 and 3A–3D for the tectonic classification. The task of obtaining classification of an unknown sample can be accomplished simply from its location in the diagrams with respect to the field boundaries, which can be reproduced by means of the coordinates (Figs. 2 and 3A–3D) given for each combination of tectonic settings.

The strategy is to plot the unknown cases in all the five diagrams and see if the samples plot in the field of the same group in all diagrams. The use of multiple diagrams is advantageous because if 85% or more of the "unknown" samples plot in the field of the same tectonic group in all the diagrams, our confidence in the correct determination of the tectonic type of the unknown will certainly increase manifold.

Conclusions

The use of the linear discriminant analysis provides a powerful, objective method of classification for basic rocks of several tectonic settings. The assignment rules suggest the use of only those variables that contribute to the power of the discriminant function, reducing the dimensionality of the problem. A comparison of the results of the training and testing sets reveals that in all cases, the rates of correct classification are consistently high for both sets (ca. 83–93%). There is not a universal diagram to fulfill all expectations, but the application of a statistical and objective method of discrimination, with field boundaries that can be reproduced, certainly provides a tool that can contribute to the reconstruction of paleotectonic settings. These new diagrams based on correctly adjusted major-element parameters on a 100% anhydrous basis using the computer program SINCLAS (Verma et al., 2002) should constitute a step forward in achieving a reliable tectonic classification system for basic rocks.

Acknowledgments

Our colleague Ignacio S. Torres-Alvarado kindly reviewed an earlier version of this paper. This work was partly supported by project PAPIIT-IN105502-3.

REFERENCES

Agrawal, S., 1995, Discrimination between late-orogenic, post-orogenic, and anorogenic granites by major element compositions: Journal of Geology, v. 103, p. 529–537.

______, 1999, Geochemical discrimination diagrams: A simple way of replacing eye-fitted field boundaries with probability based classifier surfaces: Journal of Geological Society of India, v. 54, p. 335–346.

Aitchinson, J., 1986, The statistical analysis of compositional data: London, UK, Chapman and Hall, 416 p.

______, 1989, Letter to Editor: "Measures of location of compositional data sets": Mathematical Geology, v. 21, p. 787–790.

Arculus, R. J., 1987, The significance of source versus process in the tectonic controls of magma genesis: Journal of Volcanology and Geothermal Research, v. 32, p. 1–12.

Batchelor, R. A., and Bowden, P., 1985, Petrogenetic interpretation of granitic rock series using multicationic parameters: Chemical Geology, v. 48, p. 43–55.

Chayes, F., 1987, Consistency of the two-group discrimination function in repartitioning rocks by name, *in* Size, W. B., ed., Use and abuse of statistical methods in earth sciences: New York, NY, Oxford University Press, p. 47–54.

Duncan, A., 1987, The Karoo igneous province—a problem area for inferring tectonic setting from basalt geochemistry: Journal of Volcanology and Geothermal Research, v. 32, p. 13–34.

Kendall, M. G., Stuart, A., and Ord, J. K., 1983, The advanced theory of statistics: Deeside, UK, Griffin, 780 p.

Maniar, P. D., and Piccoli, P. M., 1989, Tectonic discrimination of granitoids: Geological Society of America Bulletin, v. 101, p. 635–643.

Meschede, M., 1986, A method of discriminating between different types of mid-oceanic ridge basalts and continental tholeiites with Nb-Zr-Y diagram: Chemical Geology, v. 56, p. 207–218.

Middlemost, E. A. K., 1989, Iron oxidation ratios, norms and the classification of volcanic rocks: Chemical Geology, v. 77, p. 19–26.

Morrison, D. F., 1990, Multivariate statistical methods, 3rd ed.: New York, NY, McGraw-Hill, 495 p.

Myers, R. E., and Breitkopf, J. H., 1989, Basalt geochemistry and tectonic settings: A new approach to relate tectonic and magmatic processes, *in* Gorbatschev, R., ed., Proterozoic geochemistry: Lithos, v. 23, p. 53–62.

Pearce, J. A., 1976, Statistical analysis of major element patterns in basalt: Journal of Petrology, v. 17, p. 15–43.

______, 1982, Trace element characteristics of lavas from destructive plate boundaries, *in* Thorpe, R. S., ed., Andesites: Chichester, UK, Wiley, p. 525–548.

Pearce, J. A., and Cann, J. R., 1973, Tectonic setting of basic volcanic rocks determined using trace element analysis: Earth and Planetary Science Letters, v. 19, p. 290–300.

Pearce, J. A., Harris, N. B. W., and Tindle, A. G., 1984, Trace element discrimination diagrams for the tectonic interpretation of granitic rocks: Journal of Petrology, v. 25, p. 956–983.

Pearce, J. A., and Norry, M. J., 1979, Petrogenetic implications of Ti, Zr, Y, and Nb variations in volcanic rocks: Contributions to Mineralogy and Petrology, v. 69, p. 33–47.

Pearce, T. H., Gorman, B. E., and Birkett, T. C., 1977, The relationship between major-element chemistry and tectonic environment of basic and intermediate volcanic rocks: Earth and Planetary Science Letters, v. 36, p. 121–132.

Philpotts, J. A., 1985, Pearce-Cann discriminant diagrams applied to eastern North America Mesozoic diabase: U. S. Geological Survey Circular, v. 946, p. 114–117.

Rickwood, P. C., 1989, Boundary lines within petrologic diagrams which use oxides of major and minor elements: Lithos, v. 22, p. 247–263.

Rock, N. M. S., 1989, Reply to " Measure of location of compositional data sets": Mathematical Geology, v. 21, p. 791–793.

Sylvester, P. J., 1989, Post-collisional alkaline granites: Journal of Geology, v. 97, p. 261–280.

Thompson, R. N., Morrison, M. A., Mattey, D. P., Dickin, A. P., and Moorbath, S., 1980, An assessment of the Th-Hf-Ta diagram as discrimination for tectonomagmatic classification of crustal contaminations of magmas: Earth and Planetary Science Letters, v. 50, p. 1–10.

Vasconcelos-F., M., Verma, S. P., and Rodríguez-G., J. F., 1998, Discriminación tectónica: Nuevo diagrama Nb-Ba para arcos continentales, arcos insulares, "rifts" e islas oceánicas en rocas máficas: Boletín de la Sociedad Española de Mineralogía, v. 21, p. 129–146.

Vasconcelos-F., M., Verma, S. P., and Vargas-B., R. C., 2001, Diagrama Ti-V: Una nueva propuesta de discriminación para magmas básicos en cinco ambientes tectónicos: Revista Mexicana de Ciencias Geológicas, v. 18, p. 162–174.

Verma, S. P., 2000, Geochemistry of the subducting Cocos plate and the origin of subduction-unrelated mafic volcanism at the volcanic front of the central Mexican Volcanic Belt, *in* Delgado-Granados, H., Aguirre-Díaz, G., and Stock, J. M., eds., Cenozoic tectonics and volcanism of Mexico: GSA Special Paper 334, Geological Society of America, Boulder, Colorado, p. 195–222.

Verma, S. P., Torres-Alvarado, I. S., and Sotelo-Rodríguez, Z. T., 2002, SINCLAS: Standard igneous norm and volcanic rock classification system: Computers & Geosciences, v. 28, p. 711–715.

Verma, S. P., Torres-Alvarado, I. S., and Velasco-Tapia, F., 2003, A revised CIPW norm: Schweizerische Mineralogische und Petrographische Mitteilungen, v. 83, p. 197–216.

Wang, P., and Glover, L., III., 1992, A tectonics test of the most commonly used geochemical discriminant diagrams and patterns: Earth Science Reviews, v. 33, p. 111–131.

Whalen, J., Currie, K. L., and Chappell, B. W. 1987, A-type granites: Geochemical characteristics, discrimination, and petrogenesis: Contributions to Mineralogy and Petrology, v. 95, p. 407–419.

Whitten, E. T. H., Li, G., Bornhorst, T. J., Christenson, P., and Hicks, D. L., 1987a, Quantitative recognition of granitoid suites within batholiths and other igneous assemblages, *in* Size, W. B., ed., Use and abuse of statistical methods in earth sciences: New York, NY, Oxford University Press, p. 55–73.

Whitten, E. T. H., Bornhorst, T. J., Li, G., Hicks, D. L., and Beckwith, J. P., 1987b, Suites, subdivision of batholiths, and igneous-rock classification: Geological and mathematical conceptualization: American Journal of Science, v. 287, p. 332–352.

Wilson, M., 1989, Igneous petrogenesis: A global tectonic approach. London, UK, Unwin Hyman, 466 p.

Wood, D. A., Joron, J. L., and Treuil, M., 1979, A reappraisal of the use of trace elements to classify and discriminate between magma series erupted in different tectonic settings: Earth and Planetary Science Letters, v. 45, p. 326–336.

APPENDIX 1

Literature references for samples are included in the database according to the tectonic setting (see Table 1) and are listed alphabetically under each of the tectonic settings as follows.

Island Arc

Arculus, R. J., 1976, Geology and geochemistry of the alkali basalt-andesite association of Grenada, Lesser Antilles island arc: Geological Society of America Bulletin, v. 87, p. 612–624.

Barsdell, M., 1988, Petrology and petrogenesis of clinopyroxene-rich tholeiitic lavas, Merelava volcano, Vanuatu: Journal of Petrology, v. 29, p. 927–964.

Barsdell, M., and Berry, R. F., 1990, Origin and evolution of primitive island arc ankaramites from western Epi, Vanuatu: Journal of Petrology, v. 31, p. 747–777.

Bau, M., and Knittel, U., 1993, Significance of slab-derived partial melts and aqueous fluids for the genesis of tholeiitic and calc-alkaline island-arc basalts: Evidence from Mt. Arayat, Philippines: Chemical Geology, v. 105, p. 233–251.

Brophy, J. G., 1986, The Cold Bay volcanic center, Aleutian volcanic arc. I. Implications for the origin of high-alumina arc basalt: Contributions to Mineralogy and Petrology, v. 93, p. 368–380.

Brown, G. M., Holland, J. G., Sigurdsson, H., Tomblin, J. F., and Arculus, R. J., 1977, Geochemistry of the Lesser Antilles volcanic island arc: Geochimica et Cosmochimica Acta, v. 41, p. 785–801.

Bryan, W. B., Stice, G. D., and Ewart, A., 1972, Geology, petrography, and geochemistry of the volcanic islands of Tonga: Journal of Geophysical Research, v. 77, p. 1566–1585.

Defant, M. J., Jacques, D., Maury, R. C., De Boer, J., and Joron, J. -L., 1989, Geochemistry and tectonic setting of the Luzon arc, Philippines: Geological Society of America Bulletin, v. 101, p. 663–672.

Defant, M. J., Sherman, S., Maury, R. C., Bellon, H., de Boer, J., Davidson, J., and Kepezhinskas, P., 2001, The geology, petrology, and petrogenesis of Saba Island, Lesser Antilles: Journal of Volcanology and Geothermal Research, v. 107, p. 87–111.

Devine, J. D., 1995, Petrogenesis of the basalt-andesite-dacite association of Grenada, Lesser Antilles island arc, revisited: Journal of Volcanology and Geothermal Research, v. 69, p. 1–33.

Edwards, C., Menzies, M., and Thirlwall, M., 1991, Evidence from Muriah, Indonesia, for the interplay of supra-subduction zone and intraplate processes in the genesis of potassic alkaline magmas: Journal of Petrology, v. 32, p. 555–592.

Ewart, A., Brothers, R. N., and Mateen, A., 1977, An outline of the geology and geochemistry, and the possible petrogenetic evolution of the volcanic rocks of the Tonga-Kermadec-New Zealand island arc: Journal of Volcanology and Geothermal Research, v. 2, p. 205–270.

Foden, J. D., and Varne, R., 1980, The petrology and tectonic setting of Quaternary–Recent volcanic centres of Lombok and Sumbawa, Sunda arc: Chemical Geology, v. 30, p. 210–226.

Francalanci, L., Taylor, S. R., McCulloch, M. T., and Woodhead, J. D., 1993, Geochemical and isotopic variations in the calc-alkaline rocks of Aeolian arc, southern Tyrrhenian sea, Italy: Constraints on magma genesis: Contributions to Mineralogy and Petrology, v. 113, p. 300–313.

Hegner, E., and Smith, I. E. M., 1992, Isotopic compositions of late Cenozoic volcanics from southeast Papua New Guinea: Evidence for multi-component sources in arc and rift environments: Chemical Geology, v. 97, p. 233–249.

Hole, M. J., Saunders, A. D., Marriner, G. F., and Tarney, J., 1984, Subduction of pelagic sediments: Implications for the origin of Ce-anomalous basalts from the Marianas Islands: Journal of the Geological Society of London, v. 141, p. 453–472.

Kay, S. M., and Kay, R. W., 1994, Aleutian magmas in space and time, in Plafker, G., and Berg, H. C., eds., The geology of North America, G-1: Boulder, CO, Geological Society of America, p. 687–722.

Kay, S. M., Kay, R. W., and Citron, G. P., 1982, Tectonic controls on tholeiitic and calc-alkaline magmatism in the Aleutian arc: Journal of Geophysical Research, v. 87, p. 4051–4072.

Kita, I., Yamamoto, M., Asakawa, Y., Nakagawa, M., Taguchi, S., and Hasegawa, H., 2001, Contemporaneous ascent of within-plate type and island-arc type magmas in the Beppu-Shimabara graben system, Kyushu Island, Japan: Journal of Volcanology and Geothermal Research, v. 111, p. 99–109.

Myers, J. D., Marsh, B. D., Frost, C. D., and Linton, J. A., 2002, Petrologic constraints on the spatial distribution of crustal magma chambers, Atka volcanic center, central Aleutian arc: Contributions to Mineralogy and Petrology, v. 143, p. 567–586.

Myers, J. D., Marsh, B. D., and Sinha, A. K., 1985, Strontium isotopic and selected trace element variations between two Aleutian volcanic centers (Adak and Atka): Implications for the development of arc volcanic plumbing systems: Contributions to Mineralogy and Petrology, v. 91, p. 221–234.

Nakada, S., and Kamata, H., 1991, Temporal change in chemistry of magma source under central Kyushu, southwest Japan: Progressive contamination of mantle wedge: Bulletin of Volcanology, v. 53, p. 182–194.

Nakawa, M., Ishizuka, Y., Kudo, T., Yoshimoto, M., Hiroso, W., Ishizaki, Y., Gouchi, N., Katsui, Y., Solovyow, A. W., Steinberg, G. S., and Abdurakhmanov, A. I., 2002, Tyatya volcano, southwestern Kuril arc: Recent eruptive activity inferred from widespread tephra: The Island Arc, v. 11, p. 236–254.

Nye, C. J., and Reid, M. R., 1986, Geochemistry of primary and least fractionated lavas from Okmok volcano, central Aleutians: Implications for arc magma genesis: Journal of Geophysical Research, v. 91, p. 10,271–10,287.

Romick, J. D., Perfit, M. R., Swanson, S. E., and Shuster, R. D., 1990, Magmatism in the eastern Aleutian arc: Temporal characteristics of igneous activity on Akutan Island: Contributions to Mineralogy and Petrology, v. 104, p. 700–721.

Sakuyama, M., and Nesbitt, R. W., 1986, Geochemistry of the Quaternary volcanic rocks of the Northeast Japan arc: Journal of Volcanology and Geothermal Research, v. 29, p. 413–450.

Saunders, A. D., Tarney, J., and Weaver, S. D., 1980, Transverse geochemical variations across the Antarctic Peninsula: Implications for the genesis of calc-alkaline magmas: Earth and Planetary Science Letters, v. 46, p. 344–360.

Singer, B. S., Myers, J. D., and Frost, C. D., 1992a, Mid-Pleistocene basalt from the Seguam volcanic center, central Aleutian arc, Alaska: Local lithospheric structures and source variability in the Aleutian arc: Journal of Geophysical Research, v. 97, p. 4561–4578.

_______, 1992b, Mid-Pleistocene lavas from the Seguam volcanic center, central Aleutian arc: Closed-system fractional crystallization of a basalt to rhyodacite eruptive suite: Contributions to Mineralogy and Petrology, v. 110, p. 87–112.

Smellie, J. L., 1983, A geochemical overview of subduction-related igneous activity in the south Shetland islands, Lesser Antarctica, *in* Oliver, R. L., James, P. R., and Jago, J. B., eds., Antarctic Earthscience: New York, NY, Australian Academy of Science and Cambridge University Press, p. 352–356.

Stephenson, D., and Marshall, T. R., 1984, The petrology and mineralogy of Mt. Popa volcano and the nature of the late Cenozoic Burma volcanic arc: Journal of the Geological Society of London, v. 141, p. 747–762.

Stolz, A. J., Varne, R., Wheller, G. E., Foden, J. D., and Abbott, M. J., 1988, The geochemistry and petrogenesis of K-rich alkaline volcanics from the Batu Tara volcano, eastern Sunda arc: Contributions to Mineralogy and Petrology, v. 98, p. 374–389.

Tamura, Y., 1994, Genesis of island arc magmas by mantle derived bimodal magmatism: Evidence from the Shiraham group, Japan: Journal of Petrology, v. 35, p. 619–645.

Tatsumi, Y., Murasaki, M., Arsadi, E. M., and Nohda, S., 1991, Geochemistry of Quaternary lavas from NE Sulawesi: Transfer of subduction components into the mantle wedge: Contributions to Mineralogy and Petrology, v. 107, p. 137–149.

Tatsumi, Y., Murasaki, M., and Nohda, S., 1992, Across-arc variation of lava chemistry in the Izu-Bonin arc: Identification of subduction components: Journal of Volcanology and Geothermal Research, v. 49, p. 179–190.

Togashi, S., Tanaka, T., Yoshida, T., Ishikawa, K.-I., Fujinawa, A., and Kurasawa, H., 1992, Trace elements and Nd-Sr isotopes of island arc tholeiites from frontal arc of northeast Japan: Geochemical Journal, v. 26, p. 261–277.

Turner, S., and Foden, J., 2001, U, Th and Ra disequilibria, Sr, Nd and Pb isotope and trace element variations in Sunda arc lavas: Predominance of a subducted sediment component. Contributions to Mineralogy and Petrology, v. 142, p. 43–57.

Turner, S., Foden, J., George, R., Evans, P., Varne, R., Elburg, M., and Jenner, G., 2003, Rates and processes of potassic magma evolution beneath Sangeang Api volcano, East Sunda arc, Indonesia: Journal of Petrology, v. 44, p. 491–515.

Wheller, G. E., Varne, R., Foden, J. D., and Abbott, M. J., 1987, Geochemistry of Quaternary volcanism in the Sunda-Banda arc, Indonesia, and three-component genesis of island-arc basaltic magmas: Journal of Volcanology and Geothermal Research, v. 32, p. 137–160.

Whitford, D. J., Nicholls, I. A., and Taylor, S. R., 1979, Spatial variations in the geochemistry of Quaternary lavas across the Sunda arc in Java and Bali: Contributions to Mineralogy and Petrology, v. 70, p. 341–356.

Woodhead, J. D., 1988, The origin of geochemical variations in Mariana lavas: A general model for petrogenesis in intra-oceanic island arcs: Journal of Petrology, v. 29, p. 805–830.

Woodhead, J. D., and Johnson, R. W., 1993, Isotopic and trace-element profiles across the New Britain island arc, Papua New Guinea: Contributions to Mineralogy and Petrology, v. 113, p. 479–491.

Continental Rift

Aoki, K.-I., Yoshida, T., Yusa, K., and Nakamura, Y., 1985, Petrology and geochemistry of the Nyamuragira volcano, Zaire: Journal of Volcanology and Geothermal Research, v. 25, p. 1–28.

Auchapt, A., Dupuy, C., Dostal, J., and Kanika, M., 1987, Geochemistry and petrogenesis of rift-related volcanic rocks from South Kivi (Zaire): Journal of Volcanology and Geothermal Research, v. 31, p. 33–46.

Barberi, F., Ferrara, G., Santacroce, R., Treuil, M., and Varet, J., 1975, A transitional basalt-pantellerite sequence of fractional crystallization, the Boina centre (Afar rift, Ethiopia): Journal of Petrology, v. 16, p. 22–56.

Benito, R., López-Ruiz, J., Cebriá, J. M., Hertogen, J., Doblas, M., Oyarzum, R., and Demaiffe, D., 1999, Sr and O isotope constraints on source and crustal contamination in the high-K calc-alkaline and shoshonitic Neogene volcanic rocks of SE Spain: Lithos, v. 46, p. 773–802.

Camp, V. E., Roobol, M. J., and Hooper, P. R., 1991, The Arabian continental alkali basalt province: Part II. Evolution of Harrats Khaybar, Ithnayn, and Kura, Kingdom of Saudi Arabia: Geological Society of America Bulletin, v. 103, p. 363–391.

Class, C., Altherr, R., Volker, F., Eberz, G., and McCulloch, M. T., 1994, Geochemistry of Pliocene to Quaternary alkali basalts from the Huri Hills, northern Kenya: Chemical Geology, v. 113, p. 1–22.

Chauvel, C., and Jahn, B.-M., 1984, Nd-Sr isotope and REE geochemistry of alkali basalts from the Massif Central, France: Geochimica et Cosmochimica Acta, v. 48, p. 93–110.

Chung, S.-L., Sun, S. S., Tu, K., Chen-Hong, C., and Lee, C. L., 1994, Late Cenozoic basaltic volcanism around the Taiwan Strait, SE China: Product of lithosphere-asthenosphere interaction during continental extension: Chemical Geology, v. 112, p. 1–20.

Davidson, J. P., and Wilson, I. R., 1989, Evolution of an alkali basalt-trachyte suite from Jebel Marra volcano, Sudan, through assimilation and fractional crystallization: Earth and Planetary Science Letters, v. 95, p. 141–160.

De Mulder, M., Hertogen, J., Deutsch, S., and André, L., 1986, The role of crustal contamination in the potassic suite of the Karisimbi volcano (Virunga, African Rift Valley): Chemical Geology, v. 57, p. 117–136.

Deniel, C., Vidal, P., Coulon, C., Vellutini, P., and Piguet, P., 1994, Temporal evolution of mantle sources during continental rifting: The volcanism of Djibouti (Afar): Journal of Geophysical Research, v. 99, p. 2853–2869.

Duncker, K. E., Wolff, J. A., Harmon, R. S., Leat, P. T., Dickin, A. P., and Thompson, R. N., 1991, Diverse mantle and crustal components in lavas of the NW Cerros del Rio volcanic field, Rio Grande Rift, New Mexico: Contributions to Mineralogy and Petrology, v. 108, p. 331–345.

Fan, Q., and Hooper, P. R., 1991, The Cenozoic basaltic rocks of eastern China: Petrology and chemical composition: Journal of Petrology, v. 32, p. 765–810.

Hart, W. K., WoldeGabriel, G., Walter, R. C., and Mertzman, S. A., 1989, Basaltic volcanism in Ethiopia: Constraints on continental rifting and mantle interactions: Journal of Geophysical Research, v. 94, p. 7731–7748.

Johnson, C. M., and Lipman, P. W., 1988, Origin of metaluminous and alkaline volcanic rocks of the Latir volcanic field, northern Rio Grande rift, New Mexico: Contributions to Mineralogy and Petrology, v. 100, p. 107–128.

Le Roex, A. P., Späth, A., and Zartman, R. E., 2001, Lithospheric thickness beneath the southern Kenya rift: Implications from basalt geochemistry: Contributions to Mineralogy and Petrology, v. 142, p. 89–106.

Lee, D. -C., Halliday, A. N., Fitton, J. G., and Poli, G., 1994, Isotopic variations with distance and time in the volcanic islands of the Cameroon line: Evidence for a mantle plume origin: Earth and Planetary Science Letters, v. 123, p. 119–138.

Liu, C. -Q., Masuda, A., and Xie, G. -H., 1992, Isotope and trace-element geochemistry of alkali basalts and associated megacrysts from the Huangyishan volcano, Kuandian, Liaoning, NE China: Chemical Geology, v. 97, p. 219–231.

Luhr, J. F., Aranda-Gómez, J. J., and Housh, T. B., 1995, San Quintín volcanic field, Baja California Norte, México: Geology, petrology, and geochemistry: Journal of Geophysical Research, v. 100, p. 10,353–10,380.

Lum, C. C. L., Leeman, W. P., Foland, K. A., Kargel, J. A., and Fitton, J. G., 1989, Isotopic variations in continental basaltic lavas as indicators of mantle heterogeneity: Examples from the western U.S. Cordillera: Journal of Geophysical Research, v. 94, p. 7871–7884.

MacDonald, R., Rogers, N. W., Fitton, J. G., Black, S., and Smith, M., 2001, Plume-lithosphere interactions in the generation of the basalts of the Kenya rift, East Africa: Journal of Petrology, v. 42, p. 877–900.

McMillan, N. J., Dickin, A. P., and Haag, D., 2000, Evolution of magma source regions in the Rio Grande rift, southern New Mexico: Geological Society of America Bulletin, v. 112, p. 1582–1593.

Singer, B. S., and Kudo, A. M., 1986, Assimilation-fractional crystallization of Polvadera Group rocks in the northwestern Jemez volcanic field, New Mexico: Contributions to Mineralogy and Petrology, v. 94, p. 374–386.

Ocean Island

Bergmanis, E. C., Sinton, J. M., and Trusdell, F. A., 2000, Rejuvenated volcanism along the southwest rift zone, East Maui, Hawaii: Bulletin Volcanologique, v. 62, p. 239–255.

Chen, C. -Y., Frey, F. A., and Garcia, M. O., 1990, Evolution of alkalic lavas at Heleakala volcano, east Maui, Hawaii: Contributions to Mineralogy and Petrology, v. 105, p. 197–218.

Chen, C. Y., Frey, F. A., Garcia, M. O., Dalrymple, G. B., and Hart, S. R., 1991, The tholeiite to alkalic basalt transition at Haleakala volcano, Maui, Hawaii: Contributions to Mineralogy and Petrology, v. 106, p. 183–200.

Dupuy, C., Barsczus, H. G., Dostal, J., Vidal, P., and Liotard, J.-M., 1989, Subducted and recycled lithosphere as the mantle source of ocean island basalts from southern Polynesia, central Pacific: Chemical Geology, v. 77, p. 1–18.

Dupuy, C., Barsczus, H. G., Liotard, J. M., and Dostal, J., 1988, Trace element evidence for the origin of ocean island basalts: An example from the Austral Islands (French Polynesia): Contributions to Mineralogy and Petrology, v. 98, p. 293–302.

Frey, F. A., Garcia, M. O., and Roden, M. F., 1994, Geochemical characteristics of Koolau volcano: Implications of intershield geochemical differences among Hawaiian volcanoes: Geochimica et Cosmochimica Acta, v. 58, p. 1441–1462.

Garcia, M. O., Rhodes, J. M., Wolfe, E. W., Ulrich, G. E., and Ho, R.A., 1992, Petrology of lavas from episodes 2–47 of the Puu Oo eruption of Kilauea Volcano, Hawaii: Evaluation of magmatic processes: Bulletin of Volcanology, v. 55, p. 1–16.

Geist, D. J., McBirney, A. R., and Duncan, R. A., 1986, Geology and petrogenesis of lavas from San Cristobal Islands, Galapos Archipelago: Geological Society of America Bulletin, v. 97, p. 555–566.

Liotard, J. M., Barsczus, H. G., Dupuy, C., and Dostal, J., 1986, Geochemistry and origin of basaltic lavas from Marquesas Archipelago, French Polynesia: Contributions to Mineralogy and Petrology, v. 92, p. 260–268.

Lipman, P. W., Rhodes, R. M., and Dalrymple, G. B., 1990, The Ninole Basalt—implications for the structural evolution of Mauna Loa volcano, Hawaii: Bulletin of Volcanology, v. 53, p. 1–19.

Maaløe, S., James, D., Smedley, P., Petersen, S., and Germann, L. B., 1992, The Koloa volcanic suite of Kauai, Hawaii: Journal of Petrology, v. 33, p. 761–784.

West, H. B., Garcia, M. O., Gerlach, D. C., and Romero, J., 1992, Geochemistry of tholeiites from Lanai, Hawaii: Contributions to Mineralogy and Petrology, v. 112, p. 520–542.

Mid-Ocean Ridge

Bach, W., Erzinger, J., Dosso, L., Bollinger, C., Bougault, H., Etoubleau, J., and Sauerwein, J., 1996, Unusually large Nb-Ta depletions in North Chile ridge basalts at 36°50' to 38°56' S: Major element, trace element, and isotopic data: Earth and Planetary Science Letters, v. 142, p. 223–240.

Bach, W., Hegner, E., Erzinger, J., and Satir, M., 1994, Chemical and isotopic variations along the superfast spreading East Pacific Rise from 6 to 30°S: Contributions to Mineralogy and Petrology, v. 116, p. 365–380.

Bougault, H., Dmitriev, L., Schilling, J. G., Sobolev, A., Joron, J. L., and Needham, H. D., 1988, Mantle heterogeneity from trace elements: MAR triple junction near 18°N: Earth and Planetary Science Letters, v. 88, p. 27–36.

Bryan, W. B., Thompson, G., and Ludden, J. N., 1981, Compositional variation in normal MORB from 22°–25°N: Mid-Atlantic Ridge and Kane fracture zone: Journal of Geophysical Research, v. 86, p. 11,815–11,836.

Dosso, L., Bougault, H., Beuzart, P., Calvez, J. -Y., and Joron, J. -L., 1988, The geochemical structure of the South-East Indian Ridge: Earth and Planetary Science Letters, v. 88, p. 47–59.

Dosso, L., Bougault, H., and Joron, J. -L., 1993, Geochemical morphology of the north Mid-Atlantic Ridge, 10°–24°N: Trace element–isotope complementarity: Earth and Planetary Science Letters, v. 120, p. 443–462.

Haase, K. M., Devey, C. W., Mertz, D. F., Stoffers, P., and Dieter, G.-S., 1996, Geochemistry of lavas from Mohns Ridge, Norwegian-Greenland Sea: Implications for melting conditions and magma sources near Jan Mayen: Contributions to Mineralogy and Petrology, v. 123, p. 223–237.

Hekinian, R., Francheteau, J., Armijo, R., Cogné, J. P., Constantin, M., Girardeau, J., Hey, R., Naar, D. F., and Searle, R., 1996, Petrology of the Easter microplate region in the South Pacific: Journal of Volcanology and Geothermal Research, v. 72, p. 259–289.

Humler, E., and Whitechurch, H., 1988, Petrology of basalts from central Indian Ridge (Lat. 25°23'S, Long. 70°04'E): Estimates of frequencies and fractional volumes of magma injections in a two-layered reservoir: Earth and Planetary Science Letters, v. 88, p. 169–181.

Le Roex, A. P., and Dick, H. J. B., 1981, Petrography and geochemistry of basaltic rocks from the Conrad fracture zone on the America-Antarctica Ridge: Earth and Planetary Science Letters, v. 54, p. 117–138.

Le Roex, A. P., Dick, H. J. B., Gulen, L., Reid, A. M., and Erlank, A. J., 1987, Local and regional heterogeneity in MORB from the Mid-Atlantic Ridge between 54.5°S and 51°S: Evidence for geochemical enrichment: Geochimica et Cosmochimica Acta, v. 51, p. 541–555.

Lonsdale, P., Blum, N., and Puchelt, H., 1992, The RRR triple junction at the southern end of the Pacific–Cocos East Pacific Rise: Earth and Planetary Science Letters, v. 109, p. 73–85.

Mahoney, J., Le Roex, A. P., Peng, Z., Fisher, R. L., and Natland, J. H., 1992, Southwestern limits of Indian Ocean ridge mantle and the origin of low $^{206}Pb/^{204}Pb$ Mid-Ocean Ridge Basalt: Isotope systematics of the central southwestern Indian Ridge (17°–50°E): Journal of Geophysical Research, v. 97, p. 19,771–19,790.

Price, R. C., Kennedy, A. K., Riggs-Sneeringer, M., and Frey, F. A., 1986, Geochemistry of basalts from the Indian Ocean triple junction: Implications for the generation and evolution of Indian Ocean ridge basalts: Earth and Planetary Science Letters, v. 78, p. 379–396.

Schilling, J. -G., Zajac, M., Evans, R., Johnston, T., White, W., Devine, J. D., and Kingsley, R., 1983, Petrologic and geochemical variations along the Mid-Atlantic Ridge from 29°N to 73°N: American Journal of Science, v. 283, p. 510–586.